Eur. Phys. J. D **16**, 177–180 (2001)

THE EUROPEAN
PHYSICAL JOURNAL D
EDP Sciences

DFT studies of the molecular nanomagnet Fe_8 and the V_{15} spin system

Electronic structure and magnetic ordering

J. Kortus[1,a], M.R. Pederson[1], C.S. Hellberg[1], and S.N. Khanna[2]

[1] Center for Computational Materials Science, Naval Research Laboratory, Washington DC 20375-5000, USA
[2] Department of Physics, Virginia Commonwealth University, Richmond, VA 23284-2000, USA

Received 30 October 2000

Abstract. Based on first-principles all-electron density-functional calculations we report the electronic structure and magnetic ordering of the molecular magnet Fe_8 and the V_{15} spin system. The ferrimagnetic ordering with total spin $S = 10$ of the eight iron atoms in the Fe_8 cluster agrees well with experimental results from polarized neutron data. In comparison the low spin system V_{15} shows a spin $S = 1/2$ ground state which is also found from our calculations.

PACS. 75.50.Xx Molecular magnets – 71.24.+q Electronic structure of clusters and nanoparticles

1 Introduction

Molecular magnets such as Mn12-ac and Fe_8 are a new class of materials that have raised significant scientific interest due to the observation of quantum tunneling of magnetization and hysteresis of a purely molecular origin [1,2]. These big molecular clusters form crystals of identical nanomagnets, whose structure can be well characterized by X-diffraction measurement. Because nearly all molecules in the crystal have the same orientation, macroscopic measurement can directly observe single molecular properties and quantum phenomena. The high value of the ground state spin of $S = 10$ for Mn12-ac and Fe_8 makes these clusters also interesting for possible applications in nanoscale magnetic devices. In order to build any device it is necessary to understand the strong interactions of the metal ions, such as spin-spatial couplings and spin-spin exchange effects. Further, the ligands and other non-magnetic atoms are very important in stabilizing the spin configurations. In order to account for the strong ligand-metal interactions and to determine the electronic and magnetic structure of a given system, first-principles methods allowing for electronic, charge and structural relaxations are needed. The knowledge gained from these calculations can be very helpful for understanding and improving the systems.

One of the experimentally best studied clusters is the Fe_8-cluster with the formula $[Fe_8O_2(OH)_{12}(tacn)_6]^{8+}$, with tacn = $C_6N_3H_{15}$. The cluster is particularly interesting because its magnetic relaxation becomes temperature independent below 0.36 K, showing for the first time a pure tunneling of the magnetization [3].

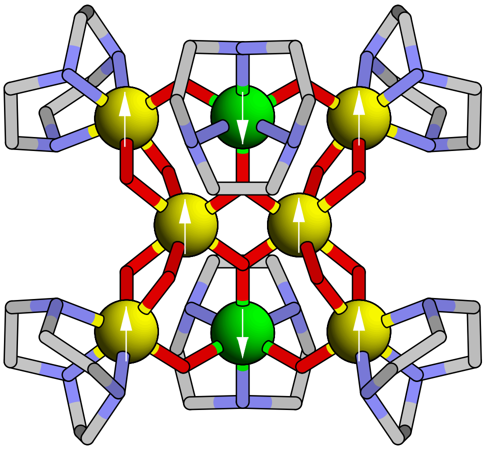
Fig. 1. The optimized geometry of the Fe_8 cluster. The balls show the iron atoms, the arrows represent the ferrimagnetic spin ordering in the cluster. The organic tacn-rings are very important for stabilizing the magnetic core of the molecule and in separating the Fe_8-clusters in the crystal. The hydrogens are not shown for clarity.

The structure of the Fe_8-cluster is shown in Fig. 1. The cluster found in molecular crystals has D_2 symmetry. The central iron atoms are connected by hydroxo bridges to the four outer iron ions. The spheres show the iron atoms, which are Fe(III) ions with a d^5 electron configuration. The ferrimagnetic coupling of spins between the eight Fe atoms results in a $S = 10$ spin ground state [4]

---

[a] e-mail: `kortus@dave.nrl.navy.mil`

and is illustrated by arrows inside the spheres. The organic tacn-rings are very important for stabilizing the magnetic core of the molecule by accepting charge, thus allowing the correct charge state of the Fe^{3+} ions. Additionally, the tacn-rings separate the Fe_8-clusters in the crystal, resulting in typical intermolecular dipole fields of the order of 0.05 T [5].

The V_{15} compound is a low spin compound with $S = 1/2$. The weakly anisotropic V_{15} demonstrates quantum behavior, such as tunneling splitting of low lying spin states and is an attractive model system for the study of mesoscopic quantum coherence and processes which destroy it. Understanding such processes is of interest to the field of quantum computing.

V_{15} has a crystallographically imposed trigonal symmetry with three sets of inequivalent vanadium atoms [6]. The unit cell contains two V_{15} clusters and is large enough that dipolar interactions between the molecules are negligible. Between 20 K and 100 K the effective paramagnetic moment is $3\mu_B$ corresponding to three independent spins and below 0.5 K it decreases showing an $S = 1/2$ ground state for the V_{15} molecule. The experimental results were interpreted with antiferromagnetic interactions between all vanadium atoms [6].

The large number of atoms in Fe_8 and V_{15} still makes first-principles calculations a challenge, and we are not aware of any other electronic structure calculations for these clusters. In this paper we present first-principles gradient corrected density-functional calculations at the all-electron level for all atoms for both the Fe_8- and the V_{15}-cluster. We report on the electronic structure and magnetic ordering for these systems.

2 Computational details

The DFT calculations [7] discussed herein were performed with the all-electron Gaussian-orbital-based NRLMOL program [8]. All calculations employed the Perdew-Burke-Ernzerhof (PBE) generalized-gradient approximation for the density-functional [9]. NRLMOL combines large Gaussian orbital basis sets, numerically precise variational integration and an analytic solution of Poisson's equation in order to accurately determine the self-consistent potentials, secular matrix, total energies and Hellmann-Feynman-Pulay forces [10]. The exponents for the single Gaussian have been fully optimized for DFT calculations [11].

2.1 Fe_8 molecular nanomagnet

Using X-ray data deposited at the Cambridge Crystallographic Data Centre [12] we generated the Fe_8 cluster.

For each Fe we used 7 *s*-like, 3 *p*-like and 2 *d*-like contracted Gaussian orbitals with 19 exponents between 0.12 and 3.87×10^6. Fluorine was described by 5 *s*- and 4 *p*-contracted orbitals using 14 bare Gaussian between 0.118 and 1.23×10^5. Oxygen had 3 *s*- and 2 *p*-contracted orbitals with 13 Gaussian between 0.105 and 6.12×10^4, nitrogen had the same number of contracted orbitals and bare Gaussian ranging from 0.12 to 5.17×10^4. Carbon had also basis of 3 *s*- and 2 *p*-orbitals with 12 exponents between 0.1 and 2.22×10^4, finally hydrogen had 2 *s*- and 1 *p*-orbital with 6 exponents between 0.1 and 77.84. This basis set resulted in a total number of 1466 contracted orbitals for the whole cluster.

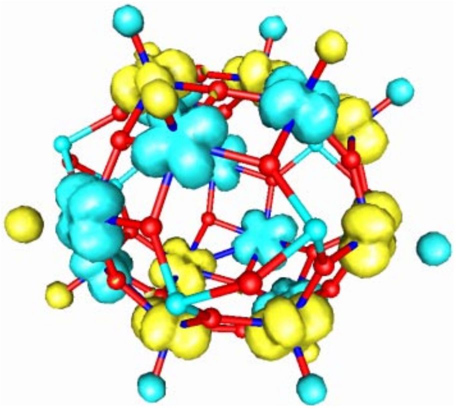

Fig. 2. The spin density of the V_{15} cluster. The picture shows clearly the single *d*-electron of a V^{4+} ion. Most of the spin density is localized at the V, less than 1% of the spin density is on the oxygen atoms which are on top of the V. The dark balls represent oxygen and the lighter ones arsenic.

2.2 V_{15} spin system

Starting from X-ray data[13] we generated several unit cells and isolated from that a single $K_6[V_{15}As_6O_{42}(H_2O)]$ unit. The structure of V_{15} is shown in Fig. 2. The vanadium atoms are at the place of the shown *d*-like orbitals, the oxygen atoms are small dark balls and the arsenic atoms are represented by lighter small balls. The potassiums included in the calculation are not shown. The three sets of the vanadium atoms define two hexagons separated by a triangle of vanadiums. Due to the layered structure the V_{15} cluster is expected to show interesting magnetic properties.

In order to use the D_3 symmetry of the V_{15} molecule [14] we initially replaced the statistically oriented water molecule in the center of the molecule by the noble gas neon. Subsequent calculations show that the electronic and magnetic properties of this system are unaffected by the presence or type of inert moiety enclosed within the void.

The basis set for vanadium consists of 20 bare Gaussian ranging from 3.108×10^6 to 0.03783 contracted to 9 *s*-, 4 *p*- and 3 *d*-molecular orbitals, for oxygen we used 13 bare Gaussian between 6.121×10^4 and 0.1049 contracted to 5 *s*-like, 3 *p*- and 1 *d*-molecular orbitals. The arsenic atoms were described by 21 bare Gaussian between 6.9614505×10^6 and 0.0607459 contracted to 10 *s*-, 5 *p*- and 4 *d*-like orbitals. This gives a total of 1853 contracted orbitals used as basis set for the calculations.

In conjunction with the conjugate-gradient algorithm the Hellmann-Feynman-Pulay forces were used in order to optimize the molecular geometry. The process was stopped after the largest nuclear gradient was smaller than 0.2 eV/Å. The total force was 0.28 eV/Å.

3 Results and discussion

3.1 Fe_8 molecular nanomagnet

In the molecular crystal [12] the positive charged Fe_8-cluster is neutralized with Br atoms. We started the calculations with Br atoms but run in problems with an incomplete charge transfer to the Br. A density of states plot revealed a strong peak of Br p-states at the Fermi level. This unchemical hybridization of the Br with the Fe_8-cluster due to energetically to high lying Br p-states can be attributed to problems with density-functional theory itself, requiring self-interaction corrections or LDA+U methods in order to account for. Another source of the problem could be the neglected water molecules in our calculations, which are present in the crystal. Calculations on a single Br-ion surrounded by water molecules showed a lowering of the Br p-states, therefore allowing for better charge transfer. The incomplete charge transfer results in a metallic density of states at the Fermi-level, which complicates the self-consistent calculations and geometry optimization of the cluster.

Even more problematic is a competition between the experimental seen ferrimagnetic state with an energetically close ferromagnetic state with also $S = 10$. Using Br atoms we could stabilize the ferrimagnetic state only by applying a small external potential on the Fe atoms favoring the ferrimagnetic state.

Due to these reasons we replaced the Br with F atoms, which are more electro-negative allowing for better charge transfer. With the F atoms the calculations converged to the experimental found ferrimagnetic state with $S = 10$ [4] without an external potential.

More recent experiments by Pontillon *et al.* [15] confirm the ferrimagnetic ordering and find smaller local moments at the two iron atoms with the minority spins than on the iron atoms with majority spins.

In order to calculate the local moments, we placed a sphere of 1.32 Å around each iron and calculated the spin density inside the sphere. Some charge will not be included in the sphere, and this approximation will give only a lower estimate for the local moments and charge states.

For the two iron atoms with minority spins we obtain a moment of $-3.6\mu_B$, whereas the majority spin irons have moments $3.8\mu_B$ and $3.9\mu_B$. These local moments are smaller than expected for Fe(III) which can be attributed to spin density outside the sphere. A plot of the spin density confirms the right spin-polarization of the irons by showing a spherical spin density around the Fe as expected for a closed shell d^5 electron configuration.

3.2 V_{15} spin system

The plot of the spin density in Fig. 2 clearly shows the localization of moment on the vanadium atoms. Even more, it clearly displays the d-character as expected for a V^{4+}-ion with a single d-electron, showing that our calculation reproduce the proper charge state of the vanadiums. The spin configuration shown in Fig. 2 has a total spin $S = 1/2$ and is also the lowest energy DFT spin configuration. This spin configuration was found by a coupled multilevel analysis which relies on fitting density-functional energies to mean-field Heisenberg energies [16].

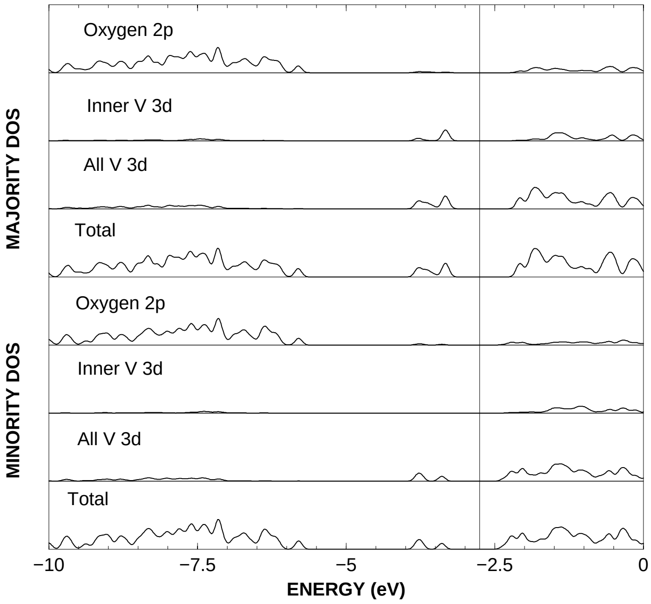

Fig. 3. Electronic density of states (DOS) broadened by 0.54 eV of V_{15} in a spin $S = 3/2$ configuration. For each spin the total DOS, the projected DOS of all V($3d$), the projected DOS of the three V($3d$) forming the inner triangle and the projected O($2p$) are presented. The vertical line divides the occupied and unoccupied states. Units are arbitrary, but the same scale has been used for all projected DOS plots.

The quantum mechanical ground state will be a superposition of all $S = 1/2$ states, therefore the obtained spin configuration from our DFT calculations can not be compared directly with experiment. Nevertheless, our results are essentially in agreement with the experimentally found $S = 1/2$ ground state [17] of the V_{15} cluster.

Figure 3 displays the density of states for a spin $S = 3/2$ configuration with ferromagnetically aligned spins in the inner triangle and antiferromagnetically coupled spins in top and bottom hexagons. This low-energy spin configuration becomes important at temperatures above 20 K and below 80 K.

For each spin the DOS is decomposed into the $3d$ contributions of all vanadium atoms (All V $3d$) and the $2p$ contributions of oxygen (Oxygen $2p$). The vanadium DOS is further decomposed into the $3d$ contribution of the vanadiums (Inner V $3d$) forming the inner triangle between the two hexagons. The projected density of states clearly shows that the states near the Fermi level are $3d$ states from the vanadium atoms.

Further, by comparing the majority and minority contributions of the vanadiums forming the inner triangle, it

Table 1. Highest occupied molecular orbital (HOMO), lowest unoccupied molecular orbital (LUMO) and spin gaps Δ for the V_{15} molecule in the spin $S = 3/2$ state. All energies are given in eV.

	HOMO	LUMO	Δ
Majority spin	−3.369	−2.159	1.210
Minority spin	−3.440	−2.412	1.082

is clear that these three vanadiums are aligned ferromagnetically since they only contribute to the majority DOS.

Further, most of the DOS in the majority DOS comes from these atoms. The states due to the V atoms at the Fermi level are well localized and do not show hybridization with other atoms such as oxygen. This indicates mainly ionic bonding, which is supported by our local moments for the vanadium atoms of $0.97\mu_B$, close to the moment of a V^{IV} ion. The DOS for the arsenic atoms is not shown, because there are no significant contributions.

In Table 1 we present the highest occupied molecular orbital (HOMO) and lowest unoccupied molecular orbital (LUMO) for the majority and minority spin channel together with the resulting spin gaps.

In order to estimate local moments we placed spheres around the atoms and calculated the spin densities inside the spheres. The only significant moments are located on the vanadium atoms, the largest other moments are at oxygen atoms with about $0.06\mu_B$. The sphere radius for the vanadium atoms was 1.32 Å. The vanadium atoms forming the two hexagons are coupled antiferromagnetically with local moments of $-0.88\mu_B$ and $0.85\mu_B$ inside the sphere. The vanadium atoms forming the middle triangle are ferromagnetically ordered with a local moment of $0.97\mu_B$. This result agrees well with the measurements above 20 K, that the spins in the triangle are localized spins on the vanadiums acting independently.

For the $S = 1/2$ spin configuration displayed in Fig. 2, the moments in the spheres do not change not significantly. They are less than 4% smaller than for the $S = 3/2$ configuration.

4 Conclusion

We performed first-principles gradient corrected density-functional calculation at the all-electron level on the experimentally interesting molecular nanomagnet Fe_8 and the spin system V_{15}. The magnetic ordering obtained from our calculations agrees well with experimental found magnetic orderings in these clusters. The local moments found for the Fe_8-cluster confirms recent experimental findings from polarized neutron scattering. In case of V_{15} we are able to describe different spin configurations. Our findings are in good agreement with experiments.

Electronic structure calculations can give insight in the magnetic interaction and help in understanding experiment. The information obtained here can be used directly for interpretation of polarized neutron scattering experiments and finding the charge state of the metal ions. Much more experimental relevant information has been obtained from our calculations as magnetic anisotropy energies, orbital moments, Heisenberg exchange parameters, hyperfine fields and vibrational properties. These will be reported elsewhere.

This work was supported in part by ONR grant N00014-98WX20709 and N0001400AF00002. Computations were performed at the DoD Major Shared Resource Centers.

References

1. J. Friedman, M.P. Sarachik, J. Tejeda, J. Maciejewski, R. Ziolo, Phys. Rev. Lett. **76**, 3820 (1996); L. Thomas, F. Lionti, R. Ballou, D. Gatteschi, R. Sessoli, B. Barbara, Nature **383**, 145 (1996).
2. C. Sangregorio, T. Ohm, C. Paulsen, R. Sessoli, D. Gatteschi, Phys. Rev. Lett. **78**, 4645 (1997).
3. W. Wernsdorfer, R. Sessoli, Science **284**, 133 (1999).
4. R. Caciuffo, G. Amoretti, A. Murani, R. Sessoli, A. Caneschi, D. Gatteschi, Phys. Rev. Lett. **81**, 4744 (1998).
5. W. Wernsdorfer, T. Ohm, C. Sangregorio, R. Sessoli, D. Mailly, C. Paulsen, Phys. Rev. Lett. **82**, 3903 (1999).
6. D. Gatteschi, L. Pardi, A.L. Barra, A. Müller, J. Döring, Nature **354**, 463 (1991).
7. P. Hohenberg, W. Kohn, Phys. Rev. **136**, B864 (1964); W. Kohn, L.J. Sham, Phys. Rev. **140**, A1133 (1965).
8. M.R. Pederson, K.A. Jackson, Phys. Rev. B **41**, 7453 (1990); K.A. Jackson, M.R. Pederson, Phys. Rev. B **42**, 3276 (1990).
9. J.P. Perdew, K. Burke, M. Ernzerhof, Phys. Rev. Lett. **77**, 3865 (1996).
10. H. Hellmann, *Einführung in die Quantentheorie* (Deuticke, Leipzig, 1937); R.P. Feynman, Phys. Rev. **56**, 340 (1939); P. Pulay, Mol. Phys. **17**, 197 (1969).
11. D. Porezag, M.R. Pederson, Phys. Rev. A **60**, 2840 (1999).
12. K. Wieghardt, K. Pohl, I. Jibril, G. Huttner Angew. Chem., Int. Ed. Engl. **23**, 77 (1984); Cambridge Crystallographic Data Centre; Refcode: COCNAJ; `http://www.ccdc.cam.ac.uk/`
13. A. Müller, J. Döring, Z. Anorg. Allg. Chem. **595**, 251 (1991).
14. A. Müller, J. Döring, Angew. Chem. Int. Ed. **27**, 1721 (1988).
15. Y. Pontillon, A. Caneschi, D. Gatteschi, R. Sessoli, E. Ressouche, J. Schweizer, E. Lelievre-Berna, J. Am. Chem. Soc. **121**, 5342 (1999).
16. J. Kortus, C.S. Hellberg, M.R. Pederson, Phys. Rev. Lett. **86**, 3400 (2001).
17. I. Chiorescu, W. Wernsdorfer, A. Müller, H. Bögge, B. Barbara, Phys. Rev. Lett. **84**, 3454 (2000).